Strawberry tree honey as a new potential functional food. Part 1: Strawberry tree honey reduces colon cancer cell proliferation and colony formation ability, inhibits cell cycle and promotes apoptosis by regulating EGFR and MAPKs signaling pathways

Sadia Afrin[a,#,1], Francesca Giampieri[b,a,#], Danila Cianciosi[a], Francesca Pistollato[b], Johura Ansary[a], Mattia Pacetti[a], Adolfo Amici[a], Patricia Reboredo-Rodríguez[b], Jesus Simal-Gandara[c], Josè L. Quiles[d], Tamara Y. Forbes-Hernández[b,*], Maurizio Battino[b,a,*]

[a]*Dipartimento di Scienze Cliniche Specialistiche ed Odontostomatologiche (DISCO)-Sez. Biochimica, Facoltà di Medicina, Università Politecnica delle Marche, 60131, Ancona, Italy*
[b]*Nutrition and Food Science Group, Dept. of Analytical and Food Chemistry, CITACA, CACTI, University of Vigo - Vigo Campus, Vigo (Spain)*
[c]*Nutrition and Bromatology Group, Department of Analytical and Food Chemistry, Faculty of Science, University of Vigo, Ourense Campus, E-32004 Ourense, Spain.*
[d]*Department of Physiology, Institute of Nutrition and Food Technology "Jose Mataix", Biomedical Research Centre, University of Granada, Spain.*

# These authors have contributed equally to this work.

*Correspondence to: Prof. Maurizio Battino, Dipartimento di Scienze Cliniche Specialistiche ed Odontostomatologiche (DISCO)-Sez. Biochimica, Facoltà di Medicina, Università Politecnica delle Marche, Ancona, Via Ranieri 65, 60131, Italy. E mail: m.a.battino@univpm.it; Tel.: +39-071-220-4646; Fax: +39-071-220-4123; Dr Tamara Y. Forbes-Hernández, Dept. of Analytical and Food Chemistry, CITACA, CACTI, University of Vigo - Vigo Campus, Vigo, 5898, Spain.

[1]Present address: Department of Gynecology and Obstetrics, School of Medicine, Johns Hopkins University, Baltimore, MD 21205, USA.

Abstract

The aim of this work was to assess the phytochemical composition and anticancer effects of Strawberry-tree honey (STH) on cellular proliferation, cell cycle and apoptosis in human colon adenocarcinoma (HCT-116) and metastatic (LoVo) cancer cells. Kaempferol and gallic acid were the major phenolic compounds. STH showed higher cytotoxic and anti-colonogenic effects in a time- and dose-dependent manner; it arrested cell cycle in S and G2/M and regulated cell cycle genes, such as cyclin D1, cyclin E, CDK2, CDK4, p21Cip, p27Kip and p-RB. STH treatment promoted apoptosis by modulating key genes (p53, caspase-3, c-PARP) as well as intrinsic (Bax/Bcl2, Cyto C and caspase-9) and extrinsic (Fas L and caspase-8) apoptotic factors. STH also caused endoplasmic reticulum stress by increasing ATF-6 and XBP-1 expressions, suppressed EGFR, HER2 and downstream markers (p-Akt and p-mTOR) and elevated p-p38MAPK and p-ERK1/2. In conclusion, STH have shown a chemo-preventive action on different colon cancer cell models.

Keywords: Strawberry tree honey; anti-proliferative properties; anti-colonogenic activities; cell cycle arrest; apoptosis activation.

1. Introduction

Nutrition has turned into an essential area in government policies after worldwide scientific community markedly established that chronic diseases, such as cancers, cardiovascular diseases and other main causes of mortality, can be slowed or inhibited by a proper consumption of nutrients and bioactive compounds rich food products (Nishida et al., 2004; Bach-Faig et al., 2011). Among various natural foods products honey is a good source of several nutritional and non-nutritional bioactive compounds, at the same time, of natural antioxidants. Honey has been accounted to show a wide variety of biological activities whereas several studies have revealed that the phenolic compounds of honey are mostly responsible for its beneficial effects of human health (Alvarez-Suarez et al., 2016; Afrin et al., 2018a; Afrin et al., 2018b; Cianciosi et al., 2018; Gasparrini et al., 2018).

Strawberry tree (*Arbutus unedo* L., Family: Ericaceae) unifloral honey (STH) is an archetypal and famous product of Mediterranean areas and its strong bitter flavor is valued by foodies and honey specialists worldwide. Conventionally it has been used generally for curative aims. Despite its importance, there is unsatisfactory information on its phytochemical characterization as well as on its beneficial functions. The raising interest of this foodstuff is not only for the diverse phenolic compositions but also for its high antioxidant capacity. Until now, only few studies have examined its physicochemical, melissopalynological and organic acid properties, and only few studies have evaluated its antioxidant and phenolic profiles, mainly phenolic acid and flavonoids (Rosa et al., 2011; Tuberoso et al., 2013; Afrin et al., 2017). The homogentisic acid (2,5-dihydroxyphenylacetic acid) is the main phenolic marker and the botanical origin marker of STH (Scanu et al., 2005), that is known for its antiradical and protection against thermal cholesterol degradation (Rosa et al., 2011).

Colorectal cancer (CRC) is the fourth main causes of cancer related death worldwide and the third most commonly diagnosed cancer (Wu et al., 2016). The available screening techniques have decreased the mortality and incidence rate, but the regular screening is still inadequate, mainly in resource-limited settings (Siegel et al., 2017). Diet rich with nutritional food and balanced lifestyle are the preventative events that have a remarkable effect in decreasing the worldwide load of CRC (Reddy, 2018). The majority of the CRC is caused by chromosomal instability, which defects the various genes related to cell proliferation, survival, cell cycle, apoptosis and DNA repair mechanisms, such as adenomatous polyposis coli, Tp53, Kirsten rat sarcoma virus oncogene (Kras), B-raf proto-oncogene (Braf), etc. (Pino & Chubg, 2010). The mitogen-activated proteins kinases (MAPKs) signaling are recognized to integrate signals from an extensive range of stimuli for controlling cellular propagation, differentiation, inflammatory responses and apoptosis in CRC (Dhillon et al., 2007). In 60% to 80% of CRC, epidermal growth factor receptor (EGFR) is overexpressed and has been connected to a number of molecular pathways such as phosphatidylinositol 3-kinase (PI3K)-protein kinase B (Akt)-mammalian target of rapamycin (mTOR) and Kras-Braf-MAPKs (Custodio & Feliu, 2013).

The efficiency of isolated compounds such as quercetin, kaempferol, luteolin, chrysin, apigenin, galangin, catechin etc. (which are the principle phenolic compounds of honey) to modulate carcinogenic processes through the alteration of different molecular targets, such as PI3K/Akt/mTOR, MAPK (p38MAPK, c-Jun N-terminal kinase (JNK) and extracellular-signal-regulated kinase 1/2 (Erk1/2)), EGFR/Kras/Braf, nuclear factor-κB (NF-κB), nuclear factor erythroid 2–related factor 2 (Nrf2) and cyclin-cyclin dependent kinase (CDK) complexes has been proven in several *in vitro* and *in vivo* CRC models (González-Vallinas et al., 2013; Lee et al.,

2011), whereby many of these targets are also represented as the backbone of modern drug discovery programs.

In this study, we investigated the anti-cancer activities of STH in human colon adenocarcinoma cells (HCT-116) and Dukes' type C, grade IV, colon metastasis cells (LoVo) by evaluating the anti-proliferative, cell cycle arresting and apoptosis activating effects through regulation of EGFR, MAPK, intrinsic and extrinsic apoptotic signaling as well as cell cycle regulatory genes.

2. Materials and methods

2.1. Honey samples, reagents and chemicals

STH samples was provided by Prof. Gavino Sanna of the Department of Chemistry and Pharmacy (University of Sassari, Italy) and kept at 4 °C until analysis. McCoy's 5A, F-12K and DMEM media for cell culture were obtained from Carlo Erba Reagents (Milan, Italy). Fetal bovine serum and antibiotic (100 IU/mL penicillin and 100 IU/mL streptomycin) were purchased from Sigma-Aldrich (Milan, Italy). Tali Apoptosis assay™ and Cell Cycle kit was bought from Invitrogen, Life Technologies. The EvaGreen 2X qPCRMaster Mix kit and the primers for real time PCR (RT-PCR) were purchased from Applied Biological Materials Inc. (Canada) and Sigma-Aldrich (Milan, Italy). The primary and secondary antibodies were obtained from Santa Cruz Biotechnology (Dallas, TX, USA) and Sigma-Aldrich (Milan, Italy). All other chemicals were purchased from Sigma-Aldrich (Milan, Italy).

2.2. Extraction, identification and quantification of STH phenolic compounds

The solid-phase extraction of phenolic compounds was performed according to previous study (Sun et al., 2016). Thermo Scientific System equipped with a Spectra SYSTEM P 4000 pump, a

Spectra SYSTEM AS 3000 auto sampler and a Finnigan Surveyor PDA Plus Detector was used for the measurement of HPLC. Chromatographic separation was carried out using a LunaC18 analytical column (150×3mm ID, 3-µm particle) with a guardcolumn (4 × 3 mm ID) containing the same packing material (Phenomenex. Torrance, CA, USA).

2.2.1. Determination of phenolic acids

An aliquot (20 µL) was injected into the column and eluted at 35°C with a constant flow rate of 0.4 mL/min. The mobile phase was composed of 2% (v/v) acetic acid in water (Component A) and of acetic acid in water and acetonitrile (1:49:50, v/v/v; Component B). The following gradient was used: 90% A for 10 min, change to 45% A in 50 min, change to 2% A in 10 min, change to 90% A in 2 min and, finally hold for 10 min giving an analysis time of 82 min. A photodiode-array detector (DAD) was employed in full-scan mode (range between 200 and 600 nm) for the determination of phenolic acids (Afrin et al., 2018c).

2.2.2. Determination of flavonols

An aliquot (20 µL) was injected into the column and eluted at 35°C with a constant flow rate of 0.4 mL/min. The mobile phase was composed of water/formic acid/acetonitrile (87:10:3), v/v/v; Component A) and water/formic acid/acetonitrile (40:10:50, v/v/v; Component B). The following gradient was used: 90% A, change to 75% A in 10 min, change to 69% A in 5 min, change to 60% A in 5 min, change to 50% A in 10 min, change to 0% in 10 min, hold for 5 min and, finally change to 90% A in 5 min giving an analysis time of 50 min. A DAD was employed in full-scan mode (range between 200 and 600 nm) for the determination of flavonols (Afrin et al., 2018c).

For quantitative analysis, stock standard solutions of individual compounds were prepared at 500 mg/L in ethanol and stored at -20°C. Multi compound working standard solutions were prepared in methanol by dilution of the stock solutions and stored in amber colored vials at -20°C. A maximum characteristic wavelength was selected as it can be seen in results section.

2.3. Total antioxidant capacity

Total antioxidant capacity of STH was assessed through Trolox equivalent antioxidant capacity (TEAC), ferric reducing antioxidant power (FRAP) and 2,4-DNP 2,2-diPhenyl-1-picrylhydrazyl (DPPH) assays, as earlier reported (Afrin et al., 2017). Results were expressed as μmol of Trolox equivalents (TE) per 100 g of honey.

2.4. Cell culture

Human colon adenocarcinoma (HCT-116), Dukes' type C, grade IV, colon metastasis (LoVo) and healthy human dermal fibroblast (HDF) cells were purchased from the American Type Culture Collection (ATCC-TIB71). McCoy's 5A medium were used for culturing HCT-116 cells, F-12K medium were used for culturing LoVo cells and DMEM medium were used for culturing HDF cells with 10% heat-inactivated fetal bovine serum, 100 IU/mL penicillin and 100 IU/mL streptomycin at 37 °C in a 5% CO_2 humidified atmosphere. For the subsequent experiment, cells were used between the 6^{th} and 10^{th} passages.

2.5. Cell proliferation assessment by MTT assay

Cell proliferation was determined with the 3-(4,5-dimethylthiazol-2-yl)-2,5-diphenyltetrazoliumbromide (MTT) assay. To evaluate the anti-proliferative effect of STH on

human colon cancer cells, cell suspensions (5×10^3/well) were seeded in 96-well plates in growth medium, overnight. Cells were treated with various concentrations of STH varied from 0 to 20 mg/mL for HCT-116 cells, 0 to 60 mg/mL for LoVo cells and 0 to 65 mg/mL for non-cancer cells for 24 to 72 h. 30 μL of RPMI medium containing 2 mg/mL of MTT was added and the cells were incubated for 2 to 4 h and the generated formazan crystals were dissolved by 100 μL of dimethylsulfoxide. The absorbance was read at 590 nm by a microplate reader (Thermo Scientific Multiskan EX, Monza, Italy) and the results were expressed by the proportion of viable cells that were computed as the absorbance of treated cells/absorbance of untreated cells ×100.

2.6. Clone formation assay

Cells at a density of 50,000 cells/well were evenly seeded on six-well plates. The cells were treated with STH (0, 3, 6, 9 and 12 mg/mL for HCT-116 cells and 0, 10, 20, 30 and 40 mg/mL for LoVo cells) for 48 h. After the incubation time, the cells were trypsinized and 1000 cells were seeded in a six-well plate and were permitted to grow for another 10 to 12 days until small colonies were visible. After washing with PBS, the visible colonies were fixed with methanol and stained with 0.2% methylene blue stain. Then, the counts of recognized colonies were manually scored and the images were recorded by a digital camera, and the results are expressed as previously described (Afrin et al., 2018d).

2.7. Cell cycle analysis

Cells were seeded in six-well plates (3.8×10^5 cells/ well) and incubated with various concentration of STH (0, 3, 6, 9 and 12 mg/mL for HCT-116 cells and 0, 10, 20, 30 and 40 mg/mL for LoVo cells) for 48 h. After the incubation, cellular pellets were fixed with 70% cold ethanol and were

put over night at -20°C. The fixed cells were washed with PBS, re-suspended in 100 µL PBS-based propidium iodide (PI) (Invitrogen™, Life Techonoliges, Milan, Italy) solution containing 0.1% Triton® X-100, 0.2 mg/ml RNase A (Invitrogen), and 20 µg/mL PI, and incubated for 30 min at room temperature into dark. Cell cycle analysis was carried out by the Tali® Cell Cycle Kit (Invitrogen™, Life Techonoliges, Milan, Italy) as earlier reported (Afrin et al., 2018c) and the results were expressed as the percentage of cells in each phase.

2.8. Determination of apoptotic cells

Cells were seeded in six-well plates (1.5×10^5 cells/ well) and incubated with various concentrations of STH (0, 3, 6, 9 and 12 mg/mL for HCT-116 cells; 0, 10, 20, 30 and 40 mg/mL for LoVo cells and 0, 12 and 40 mg/mL for healthy cells) for 48 h. After that, cellular pellets were re-suspending with 100 µL of Annexin binding buffer (ABB) and 5 µL of Annexin V Alexa Fluor® 488 and incubated for 20 min at room temperature into the dark. Again pellets were centrifuged for removing the excess mixture and re-suspending with 100 µL of ABB and 1 µL of Tali™ PI, and incubated 1 to 5 min at room temperature into dark before reading the sample by Tali™ Cellular Analysis Slide's chamber and analyzed in the Tali™ Image-Based Cytometer (Invitrogen™, Life Techonoliges, Milan, Italy). The annexin V-negative/PI negative cells were identified as viable cells and the annexin-V positive/ PI negative cells were recognized as apoptotic cells whereas the annexin V positive/ PI positive cells were identified as dead cells (Giampieri et al., 2018).

2.9. RNA isolation and real time PCR

Cells were treated with various concentrations of STH (0, 3, 6, 9 and 12 mg/mL for HCT-116 cells and 0, 10, 20, 30 and 40 mg/mL for LoVo cells) for 48 h. Total RNA content of cells was isolated

using a PureLink® RNA Mini Kit (Invitrogen, Carlsbad, CA, USA) and cDNA was synthesis following reverse transcription (5X All-In-One RT MasterMix kit, Applied Biological Materials Inc. Canada) according to the manufacturer's protocol. RT-PCR was carried out using EvaGreen 2X qPCR MasterMix (EvaGreen 2X qPCR MasterMix kit, Applied Biological Materials Inc. Canada) of forward and reverse primers **(Table 1)** of cell cycle regulatory genes (CDK2, CDK4, cyclin D1, cyclin E, p21waf1/cip1, p27kip1, phosphorylated (p)-retinoblastoma (Rb)) and apoptotic genes (p53, caspase-3, -8, -9, cleaved-Poly (ADP-ribose) polymerase (c-PARP), B-cell lymphoma-2 (Bcl-2), Bcl-2 associated X protein (Bax), cytochrome c (Cyt c), fatty acid synthase ligand (FasL)) on a RT-PCR system (Corbett Life Science, Rotor-Gene 3000, Mortlake, Australia). Glyceraldehyde-3-phosphate dehydrogenase (GADPH) was used for normalizing quantitative data and the $2^{-\Delta\Delta ct}$ method was used for calculating while the results expressed by fold change.

2.10. Western blotting

Protein extraction of cellular pellet was performed by previously described method (Afrin et al., 2018d). By using 8 to 10% polyacrylamide gel, proteins are separated and transferred into a nitrocellulose membrane with the help of the trans-blot SD semidry electrophoretic transfer cell (Bio-Rad, Hercules, CA, USA). The membranes were blocked with Tris HCl buffered saline with Tween 20 (TBST) and with 5% non-fat-milk for 1 h at room temperature. The primary antibodies p53, caspase-3, c-PARP, activating transcription factor 6 (ATF6), X-box-binding protein 1 (XBP1), EGFR, human epidermal growth factor receptor 2 (HER2), p-Akt, p-mTOR, p-p38MAPK, p-Erk1/2 and GADPH, were used after at 4°C incubation, overnight. Membranes were washed with TBST and again incubated with secondary antibodies for another 1h. Immunolabeled proteins were recognized by using a chemiluminescence method (C-DiGit Blot Scanner, LICOR,

Bad Homburg, Germany) and bands density were quantified by image studio digits software 3.1 (C-DiGit Blot Scanner, LICOR, Bad Homburg, Germany).

2.11. Statistical analysis

Data were expressed as mean ± standard deviation (SD) of three independent experiments. Statistical analysis was performed by using one-way analysis of variance (ANOVA) followed by Tukey's honestly significant difference (HSD) post hoc test (*P < 0.05, **P < 0.01 and ***P < 0.0001, compared to the control group and $^{\#}p< 0.05$; $^{\#\#}p< 0.01$ compared to the treatment group).

3. Results

3.1. Phenolic profile and total antioxidant capacity of STH

In the present study, we observed 12 phenolic compounds in STH that are listed in **Table 2**. All concentrations were calculated using the calibration curve of each analyte. Two different families have been determined: flavonols including rutin, myricetin, fisetin, quercetin, luteolin, apigenin, kaempferol and isorhammetin and phenolic acids including gallic acid, protocatechuic acid, 4-hydroxybenzoic acid, vanillic acid, caffeic acid, syringic acid, *p*-coumaric acid, *trans*-ferulic acid, ellagic acid and *trans*-cinnamic acid **(Figure 1)**. It was found that gallic acid and kaempferol were the main components (3.92 and 1.90 mg/100 g honey, respectively). Other flavonols (quercetin and luteolin; 0.90 and 0.79 mg/100 g honey, respectively) and phenolic acids (4-hydroxybenzoic acid and caffeic acid; 1.29 and 1.22 mg/100g honey, respectively) were presented in low concentrations.

Furthermore, total antioxidant capacity of STH was quantified by TEAC, FRAP, and DPPH assays. The values were 392.13±0.45µmol TE/100g for TEAC, 539.01±0.27µmol TE/100 g for FRAP, and 200.83±0.68 µmol TE/100 g for DPPH (**Table 3**).

3.2. Anti-proliferative effects of STH in colon cancer cells

The colon cancer HCT-116 and LoVo cells were treated with various concentration of STH for 24 to 72 h and their viability was assessed by MTT assay. As shown in **Figure 2A and 2B**, STH decreased the viability of both colon cancer cells in a dose and time-dependent manner. In HCT-116 cells, the cytotoxic effect was more prominent at less concentration **(Figure 2A),** but in LoVo cells, only the high concentrations of STH induced cytotoxic effects because of the metastatic nature of this cell lines **(Figure 2B)**. In the case of non-cancer cells, STH treatment did not induce any toxicity up to 45 mg/mL for 72 h **(Figure 2C)**, which was highly toxic for the both colon cancer cells.

As such, for HCT-116 cells, the STH concentrations of 3, 6, 9 and 12 mg/mL at 48 h were selected for further experiments, while for LoVo cells the chosen concentrations were 10, 20, 30 and 40 mg/mL at 48 h. These concentrations led to a cell viability from 80% to 40%. Additionally, in healthy fibroblast cells, the highest concentration of STH (12 mg/mL and 40 mg/mL) used for the both cancer cell lines were chosen to investigate the cytotoxic effects of STH on non-cancer cells.

3.3. Anti-clonogenic effects of STH in colon cancer cells

The colony formation assay is a well-established method to determine the *in vitro* malignant transformation in cells. As shown in **Figure 3A and 3B,** STH treatment decreased the colony formation in HCT-116 cells up to 86% at the highest concentration (12 mg/mL) while in LoVo cells, the colony formation decreased up to 77% at the concentration of 40 mg/mL compared to control (0 mg/mL). Moreover, in non-cancer cells **(Figure 3C)**, STH exposure increased the colony formation up to 225% at the concentration of 12 mg/mL and 126% at the concentration of 40 mg/mL compared to control (0 mg/mL).

3.4. STH treatments exerts cell cycle arrest in colon cancer cells

One of the most attractive target in cancer therapy is the modulation of cell cycle progression. The percentage of cells in each phase of cell cycle was determined by flow cytometry analysis after STH treatment **(Figure 4)**. In HCT-116 cells, STH treatment arrested the cell cycle at S phase by significantly ($p < 0.01$) increasing the accumulation of cells up to 56% compared to control (23%) and the effects were dose dependently, while the percentage of cells at G1 and G2/M phase were decreased **(Figure 4A)**. Furthermore, in LoVo cells, STH treatment arrested the cell cycle at G2/M phase by accumulating up to 30% of cells compared to control 9% and at the same time percentage of cells at G1 and S phase were decreased in a dose-dependent way **(Figure 4B)**.

3.5. Modulations of cell cycle regulatory genes after STH treatment

The regulation process of cell cycle is controlled by several CDKs which bind with their cyclin subunits, modulating the CDK inhibitors (p21Cip and p27Kip) and phosphorylating the Rb genes for activation of the cell cycle regulatory genes (Vermeulen, Van Bockstaele & Berneman, 2003). The results shown in **Figure 4** confirmed that the STH treatment arrested the cell cycle in both colon cancer cells.

Furthermore, we observed the cell cycle regulatory genes (CDK2, CDK4, cyclin D1, cyclin E, p21Cip1, p27kip1 and p-Rb) expression after the STH exposure **(Figure 5)**. In HCT-116 cells, STH treatment significantly ($p < 0.01$) suppressed the expression of CDK2 up to 0.67 fold, CDK4 up to 0.54 fold, cyclin D1 up to 0.64 fold, cyclin E up to 0.48 fold and p-Rb up to 0.55 fold at the highest concentration compared to control (1.00 fold) **(Figure 5A)**. At the same time, the expression of p21Cip and p27kip significantly ($p < 0.01$) increased up to 1.77 fold and 1.61 fold. Vice versa, in LoVo cells, no changes were observed in the expression of CDK2, CDK4 and cyclin

E after STH treatment, while increased p21Cip1 up to 1.83 fold and p27Kip1 up to 2.06 fold, and decreased cyclin D1 up to 0.57 fold and p-Rb up to 0.42 fold expressions were observed **(Figure 5B)**. Therefore, STH arrested the cell cycle at S phase through decreasing the mRNA expression of cyclin D1, cyclin E, CDK2, CDK4, p-Rb and increasing p21Cip and p27Kip expressions in HCT-116 cells. In LoVo cells, STH arrested the cell cycle at G2/M phase by suppressing the expression of cyclin D1 and p-Rb and at the same time increasing p21Cip and p27Kip expressions, respectively.

3.6. Induction of apoptosis by STH in colon cancer cells

Activation of apoptosis is a well-established method for exerting anti-cancer effects. STH treatment significantly increased the number of apoptotic cells in a dose-dependent way in both colon cancer cells **(Figure 6)**. In HCT-116 cells, the percentage of apoptotic cells was 25% after STH exposure (12 mg/mL) compared to control 7% (0 mg/mL) and the numbers of dead cells were increased up to 60%, respectively, compared to untreated cells 84% **(Figure 6A)**. Inversely, the number of live cells was significantly ($p < 0.01$) decreased up to 20% compared to control 5% at the highest concentration of STH **(Figure 6A)**. Additionally, in LoVo cells, we observed the 18% of apoptotic cells after STH treatment while in the control it was 2% **(Figure 6B)**. The number of live cells was decreased in a dose-dependent manner up to 47% compared to control 83% and vice versa, the dead cells number increased up to 34% while the number of untreated cells was 8% (**Figure 6B)**. Furthermore, we observed the apoptotic effects of STH in non-cancer cells and examined no statistical difference compared to control while at the concentration 40 mg/mL very few effects were observed on the number of live cells (decreased) and dead cells (increased) **(Figure 6C)**.

3.7. STH exerts intrinsic and extrinsic apoptosis and ER stress on colon cancer cells

For confirming the apoptosis activation, the levels of several intrinsic and extrinsic markers were analyzed by RT-PCR on HCT-116 and LoVo cells untreated or treated for 48h with STH **(Figure 7)**. The expression of all the apoptotic markers were increased dose-dependently: p53 increased up to 3.26 fold for HCT-116 cells and 1.76 fold for LoVo cells, Bax/Bcl-2 increased up to 3.06 fold for HCT-116 cells and 5.01 fold for LoVo cells, Cyto C increased up to 1.25 fold for HCT-116 cells and 3.50 fold for LoVo cells, FasL increased up to 1.83 fold for the both cells, caspase-3 increased up to 1.55 fold for HCT-116 cells and 1.81 fold for LoVo cells, caspase-8 increased up to 1.34 fold for HCT-116 cells and 1.80 fold for LoVo cells, caspase-9 increased up to 1.36 fold for HCT-116 cells and 2.26 for LoVo cells and c-PARP increased up to 3.10 fold for HCT-116 cells and 1.77 fold for LoVo cells, respectively.

Subsequently, the gene expression of three main apoptotic markers p53, caspase-3 and c-PARP were further investigated at protein level by western blotting **(Figure 8A and 8B)**. The results confirmed more than 2-fold upregulation of p53 (2.35 fold for HCT-116 cells and 2.27 fold for LoVo cells), caspase-3 (2.16 fold for HCT-116 cells and 3.09 fold for LoVo cells) and c-PARP (2.33 fold for HCT-116 cells and 2.70 fold for LoVo cells) expression after the highest doses of STH compared to untreated control.

Activation of ER stress is also associated for the induction of apoptosis; we further investigated the probable alteration of ATF6 and XBP1 protein expression on colon cancer cells after STH treatment **(Figure 8C and 8D)**. In HCT-116 cells, the expression of ATF6 and XBP1 increased up to 2.27 fold and 2.12 fold while in LoVo cells it increased up to 2.45 fold and 2.34 fold at the highest concentrations.

3.8. STH modulates expression of EGFR and MAPK signaling pathways on colon cancer cells

The anti-cancer effects of STH on HCT-116 and LoVo cells were also evaluated at the molecular levels by examining the protein expression of several genes related to proliferation, survival and apoptosis. STH treatment significantly ($p < 0.01$) altered the expression of EGFR, HER2 and downstream target p-Akt, p-mTOR on both colon cancer cells treated or untreated for 48h with STH **(Figure 9A and 9B)**. EGFR (up to 0.52 fold for HCT-116 cells and 0.41 fold for LoVo cells), HER2 (up to 0.55 fold for HCT-116 cells and 0.57 fold for LoVo cells), p-Akt (up to 0.44 fold for HCT-116 cells and 0.41 fold for LoVo cells) and p-mTOR (up to 0.51 fold for HCT-116 cells and 0.43 fold for LoVo cells) were down-regulated. Strongest up-regulation was observed at p-p38MAPK (up to 2.25 fold for HCT-116 cells and 1.87 fold for LoVo cells) and p-ERK1/2 (up to 3.40 fold for HCT-116 cells and 2.09 fold for LoVo cells) and the effects were more prominent in HCT-116 cells compared to LoVo cells **(Figure 9C and 9D)**.

4. Discussion

In the last decade, there is an increasing interest on the consumption of the antioxidant rich food stuffs because of their protective role against different chronic diseases such as cancer (Pandey & Rizvi, 2009).

Table 2 shows the phenolic compounds identified in STH. With respect to flavonols, kaempferol represents 41.12% of the total flavonols identified. On the other hand, gallic acid is the main phenolic acid representing 54.44% of the total phenolic acids. Two previous studies addressed the characterization of the phenolic composition in STH. Petretto et al., (2015) studied the phenolic composition (flavonols and phenolic acids) on ten monofloral honeys by HPLC-DAD analysis. In agreement with the present study, kaempferol and luteolin were the main flavonols identified in

STH, showing a concentration of 1.06 and 0.96 mg/100 g of honey, respectively. In another study, Tuberoso et al., (2013) determined two phenolic compounds in STH (homogentisic acid and gallic acid).

The antioxidant capacity of STH was moderately lower compared to the capacity accounted in a previous study (Tuberoso et al., 2013). It is noted that STH presented higher antioxidant capacity (**Table 3**) compared to well-known honey such as Manuka honey (Afrin et al., 2017), Portuguese honey (Ferreira et al., 2009), Cuban honey (Alvarez-Suarez et al., 2010), and Malaysian honey (Kishore et al., 2011). According to the previous studies, a significant correlation was observed between the phenolic parameters and the antioxidant capacity (Afrin et l., 2017; Kishore et al.,2011).

To the best of our knowledge, this is the first report to demonstrate the anti-proliferative and apoptotic effects of STH on colon cancer cells. As shown above, STH is able to significantly decrease the proliferation and colony formation of colon cancer HCT-116 and LoVo cells, while at the same concentrations, it is not toxic in non-cancer cells **(Figure 2** and **Figure 3)**. The anti-proliferative results of other types of honey such as Manuka (Afrin et al., 2018c), Nenas and Gelam (Wen et al., 2012) honeys used concentration were 2 to 8 times higher compared the concentration of STH used in this study. This dissimilarity is mostly due to the honey phenolic composition, which depends on this floral and geographical origin. The representative major phenolic compounds of STH **(Table 2)**, such as flavonols: kaempferol, quercetin, and luteolin, and phenolic acid: gallic acid, caffeic acid, ferulic acid and cinnamic acid are well recognized for their chemopreventive effects on colon cancer by preventing initiation to progression stages whereas some of the phenolic compounds are already on phase II and phase III clinical trial (González-Sarrías et al., 2015; Afrin et al., 2018e).

Cell cycle arrest is one of the effectual strategies to prevent uncontrolled cell proliferation. Therefore, we evaluated the mode of action of STH to prevent cancer progression by arresting cell cycle. Our results showed that dose-dependently, STH caused cell cycle arrest in S phase of HCT-116 cells and G2/M phase for LoVo cells **(Figure 4)**. Previous studies reported that Manuka honey (Afrin et al.,2018c) or representative phenolic compounds of honey, such as cinnamic acid (Anantharaju et al., 2017), ellagic acid (González-Sarrías et al., 2016), apigenin (Wang et al., 2000) etc. has also been accounted to elicit S and G2/M phase cell cycle arrest in HCT-116, Caco-2, SW480 and HT-29 colon cancer cells. Cyclin-CDK complex are the main regulators for the cell cycle progressions whereas the CDK inhibitors, p21Cip and p27Kip promotes the cell cycle arrest (Vermeulen, Van Bockstaele & Berneman, 2003). We evaluated that STH exposure dose-dependently and significantly decreased the mRNA levels of CDK2, CDK4, cyclin D1 and cyclin E for HCT-116 at S phase and only cyclin D1 for LoVo cells at G2/M phase **(Figure 5)**. In addition, STH significantly increased the levels of p21Cip and p27Kip, as well as decreased the p-Rb levels for both colon cancer cells. There are a good number of studies on natural compounds and colon cancer cells that support our present results. For example, cinnamic and gallic acid arrest the cell cycle at S and G2/M phase through increasing p21 expression (Anantharaju et al., 2017; González-Sarrías et al., 2016), flavokawain c arrest at S phase by decreasing cyclin E, CDK2, CDK4, p-Rb and increasing p21Cip and p27Kip expression (Phang et al., 2016) as well as flavonols arrest at G2/M phase by reducing cyclin D1 expressions (Gómez-Alonso et al., 2012).

Apoptosis induction is another vital approach for controlling cancer cells growth. Several natural compounds that activated apoptosis by regulating the apoptotic signals have the potentiality for cancer prevention (Elmore, 2007). In the present study, STH increased the accumulation of apoptotic and dead cells number and at the same time decreased the number of live cells in both

HCT-116 and LoVo cells and the effects were dose-dependent **(Figure 6)**. These results were reliable with earlier reports showing that honey or bee products induced cellular apoptosis in several cancer cells (Afrin et al., 2018c; Giampieri et al., 2018; Kang et al., 2017).

P53 is one of the main apoptosis signaling pathways consist of the p53 tumor suppressor and this protein is a nuclear transcription factor that controls the expression of a wide-ranging of genes implicated in apoptosis, DNA repair and growth arrest in response to drug (Fridman and Lowe, 2003). In addition, caspase-3 play a key role in the implementation of the apoptotic program, is mainly accountable for the cleavage of PARP through cell death process (Nicholson et al. 1995). The molecular mechanism by which STH induced apoptosis induction was further evaluated by the expression of p53, caspase-3 and c-PARP. Activation of tumor suppressor p53, main caspase protein caspase-3 and its downstream targets c-PARP confirmed the STH induction of apoptosis in both HCT-116 and LoVo colon cancer cells **(Figure 8)**. Furthermore, STH treatment elevated the levels of Bax/Bcl2, Cyto C and caspase-9 in a dose-dependent manner activating intrinsic pathway, as well as Fas L and caspase-8, activating extrinsic apoptotic pathways **(Figure 7)**. Existing data support that the honey phenolic compounds such as luteolin (Kang et al., 2017), quercetin (Kee et al., 2016), myricetin (Kim et al., 2014), kaempferol (Wang et al., 2018), caffeic acid (Tang et al., 2017) etc. mediated their anti-cancer effects by activating intrinsic and extrinsic apoptotic pathway.

There is a strong relation between ER-stress and apoptosis increasing the therapeutic efficacy through eliminating the injured cells (Sano & Reed, 2013). Our results demonstrated that STH treatment increased the expression of ATF6 and XBP1 in both colon cancer cells **(Figure 8)**. These findings were consistent with earlier reports showing that quercetin induced apoptotic cell death

by activating ATF6, XBP1 and other ER stress markers on HCT-116 colon cancer cells (Khan et al., 2016).

The EGFR/HER2 and its downstream signaling pathway p-Akt and p-mTOR represent an attractive anti-carcinogenic target which plays a significant role for the progression of colon cancer by initiating cell survival, proliferation, apoptosis, invasion, angiogenesis as well as metastasis (Custodio & Feliu, 2013). Caffeic acid and kaempferol suppress the expression of EGFR (Wu et al., 2011), p-Akt and p-mTOR (Chiang et al., 2014; Wang et al., 2018) pathways, exerting anti-proliferative effects and activating apoptosis in several cancer models. In agreements with previous studies, we showed that STH could potentially suppressed the colon cancer cells proliferation and inducing apoptosis by inhibiting the expression of EGFR, HER2, p-Akt and p-mTOR **(Figure 9)**. The p38MAPK and p-ERK1/2 are the major markers of MAPK signaling which prompts a large number of signal associated with proliferation, apoptosis, differentiation as well as inflammation on several carcinogenic pathways (Zhang & Liu, 2002). We examined that STH treatment increased in a dose-dependent way the expression of p-p38MAPK and p-ERK1/2 in HCT-116 and LoVo cancer cells **(Figure 9)**. In agreement with our results, similar efficacy was observed after luteolin treatment on HT-29 cells (Kang et al., 2017) and quercetin treatment on CT-29 cells (Kee et al., 2016); both studies found that the MAPK activation was responsible for the induction of apoptosis.

5. Conclusion

Our results provide evidence that STH induced anti-proliferative effects in HCT-116 and LoVo through reducing colony formation ability and suppressing the expression of EGFR, HER2 and corresponding markers p-Akt and p-mTOR. Exposure of STH induced cell cycle arrest at the S

phase in HCT-116 cells and G2/M phase in LoVo cells, leading to regulate the mRNA levels of cell cycle regulatory genes. In addition, STH induced apoptosis in both cancer cells through activating the intrinsic and extrinsic pathways, increasing the ER stress and elevation of MAPK signaling. Currently, we are trying to observe the oxidative stress induced cancer cells death, metabolic alteration and chemo-sensitizing effects of STH on colon cancer cells. This is an initial step to observe the biological as well as the anti-cancer effects of STH. All this observation provides the fundamental approaches into the molecular mechanism of STH induced cancer cell death, reinforcing the interest for this foodstuff for the prevention and management of colon cancer. Additionally, this study also highly encourages to examine the most important single compound in STH depending on the effectiveness of growth suppression and apoptosis induction on cancer cells.

Acknowledgements

The author would like to thank Prof. Gavino Sanna, Department of Chemistry and Pharmacy (University of Sassari, Italy), for providing STH samples.

Conflict of interest

The authors declare no conflicts of interest.

References

Afrin, S., Forbes-Hernandez, T.Y., Gasparrini, M., Bompadre, S., Quiles, J.L., Sanna, G., Spano, N., Giampieri, F., Battino, M. (2017). Strawberry-tree honey induces growth inhibition of human

colon cancer cells and increases ROS generation: a comparison with Manuka honey. *International Journal of Molecular Sciences, 18,* 613.

Afrin, S., Giampieri, F., Forbes-Hernandez, T.Y., Gasparrini, M., Amici, A., Cianciosi, D., Quiles, J.L., Battino M. (2018a). Manuka honey synergistically enhances the chemopreventive effect of 5-fluorouracil on human colon cancer cells by inducing oxidative stress and apoptosis, altering metabolic phenotypes and suppressing metastasis ability. *Free Radical Biology and Medicine*, *126*, 41-54.

Afrin, S., Gasparrini, M., Forbes-Hernández, T.Y., Cianciosi, D., Reboredo-Rodriguez P., Manna, P.P., Battino, M., Giampieri, F. (2018b). Protective effects of Manuka honey on LPS-treated RAW 264.7 macrophages. Part 1: Enhancement of cellular viability, regulation of cellular apoptosis and improvement of mitochondrial functionality. *Food and Chemical Toxicology, 121*, 203-213.

Afrin, S., Giampieri, F., Gasparrini, M., Forbes-Hernandez, T.Y., Cianciosi, D., Reboredo-Rodríguez, P., Amici, A., Quiles, J.L., Battino M. (2018c). The inhibitory effect of Manuka honey on human colon cancer HCT-116 and LoVo cell growth. Part 1: the suppression of cell proliferation, promotion of apoptosis and arrest of the cell cycle. *Food & Function*, *9,* 2145-2157.

Afrin, S., Giampieri, F., Gasparrini, M., Forbes-Hernandez, T.Y., Cianciosi, D., Reboredo-Rodríguez, P., Manna, P.P., Zhang, J., Quiles, J.L., Battino, M. (2018d). The inhibitory effect of Manuka honey on human colon cancer HCT-116 and LoVo cell growth. Part 2: Induction of oxidative stress, alteration of mitochondrial respiration and glycolysis, and suppression of metastatic ability. *Food & Function, 9,* 2158-2170.

Afrin, S., Giampieri, F., Gasparrini, M., Forbes-Hernández, T.Y., Cianciosi, D., Reboredo-Rodriguez, P., Zhang, J., Manna, P.P., Daglia, M., Atanasov, A.G. and Battino, M. (2018e). Dietary phytochemicals in colorectal cancer prevention and treatment: a focus on the molecular mechanisms involved. *Biotechnology advances*, DOI: https://doi.org/10.1016/j.biotechadv.2018.11.011

Alvarez-Suarez, J.M., Giampieri, F., Cordero, M., Gasparrini, M., Forbes-Hernández, T.Y., Mazzoni, L., Afrin, S., Beltrán-Ayala, P., González-Paramás, A.M., Santos-Buelga, C. (2016). Activation of AMPK/Nrf2 signalling by Manuka honey protects human dermal fibroblasts against oxidative damage by improving antioxidant response and mitochondrial function promoting wound healing. *Journal of Functional Foods, 25,* 38-49.

Alvarez-Suarez, J.M., Tulipani, S., Díaz, D., Estevez, Y., Romandini, S., Giampieri, F., Damiani, E., Astolfi, P., Bompadre, S., Battino, M. (2010). Antioxidant and antimicrobial capacity of several monofloral Cuban honeys and their correlation with color, polyphenol content and other chemical compounds. *Food and Chemical Toxicology, 48,* 2490-2499.

Anantharaju P.G., Reddy D.B., Padukudru M.A., Chitturi C.H.M.K., Vimalambike M.G., Madhunapantula S.V. (2017). Induction of colon and cervical cancer cell death by cinnamic acid derivatives is mediated through the inhibition of Histone Deacetylases (HDAC). *PLoS One, 12*, e0186208.

Bach-Faig, A., Berry, E.M., Lairon, D., Reguant, J., Trichopoulou, A., Dernini, S., Medina, F.X., Battino, M., Belahsen, R., Miranda, G., Serra-Majem, L., Mediterranean Diet Foundation Expert

Group., (2011). Mediterranean diet pyramid today. Science and cultural updates. *Public Health Nutr*ition, *14*, 2274-2284.

Chiang, E.P.I., Tsai, S.Y., Kuo, Y.H., Pai, M.H., Chiu, H.L., Rodriguez, R.L., Tang F.Y., (2014). Caffeic acid derivatives inhibit the growth of colon cancer: involvement of the PI3-K/Akt and AMPK signaling pathways. *PLoS One, 9,* e99631.

Cianciosi, D., Forbes-Hernández, T.Y., Afrin, S., Gasparrini, M., Reboredo-Rodriguez, P., Manna, P., Zhang, J., Bravo Lamas, L., Martínez Flórez, S., Agudo Toyos, P. (2018). Phenolic Compounds in Honey and Their Associated Health Benefits: A Review. *Molecules, 23*, 2322.

Custodio, A., Feliu, J. (2013). Prognostic and predictive biomarkers for epidermal growth factor receptor-targeted therapy in colorectal cancer: beyond KRAS mutations. *Critical Reviews in Oncology/Hematology, 85*, 45-81.

Dhillon, A.S., Hagan, S., Rath, O., Kolch, W. (2007). MAP kinase signalling pathways in cancer. *Oncogene, 26,* 3279.

Elmore S. (2007). Apoptosis: a review of programmed cell death. *Toxicologic Pathology, 35*, 495-516.

Ferreira, I.C.F.R., Aires, E., Barreira, J.C.M., Estevinho, L.M. (2009). Antioxidant activity of Portuguese honey samples: Different contributions of the entire honey and phenolic extract. *Food Chemistry, 114*, 1438-1443.

Fridman, J. S., & Lowe, S. W. (2003). Control of apoptosis by p53. *Oncogene, 22*, 9030.

Gasparrini, M., Afrin, S., Forbes-Hernández, T.Y., Cianciosi, D., Reboredo-Rodriguez, P., Amici, A., Battino, M., Giampieri, F. Protective effects of Manuka honey on LPS-treated RAW 264.7 macrophages. Part 2: Control of oxidative stress induced damage, increase of antioxidant enzyme activities and attenuation of inflammation. *Food and Chemical Toxicology*, *120*, 578-587.

Giampieri, F., Quiles, J.L., Orantes-Bermejo, F.J., Gasparrini, M., Forbes-Hernandez, T.Y., Sánchez-González, C., Llopis, J., Rivas-García, L., Afrin, S., Varela-López, A., Cianciosi, D., Reboredo-Rodriguez, P., Fernández-Piñar, C.T., Iglesias Ruben, C., Ruiz, R., Aparicio, S., Crespo, J., Lopez, D.L., Xiao, J., Battino M. (2018). Are by-products from beeswax recycling process a new promising source of bioactive compounds with biomedical properties. *Food and Chemical Toxicology*, *112*, 126-133.

Gómez-Alonso S., Collins V.J., Vauzour D., Rodríguez-Mateos A., Corona G., Spencer J.P.E. (2012). Inhibition of colon adenocarcinoma cell proliferation by flavonols is linked to a G2/M cell cycle block and reduction in cyclin D1 expression. *Food Chemistry, 130*, 493-500.

González-Sarrías, A., Núñez-Sánchez M.Á., Tomé-Carneiro J., Tomás-Barberán F.A., García-Conesa M.T., Espín J.C. (2016). Comprehensive characterization of the effects of ellagic acid and urolithins on colorectal cancer and key-associated molecular hallmarks: MicroRNA cell specific induction of CDKN1A (p21) as a common mechanism involved, *Molecular Nutrition & Food Research, 60*, 701-716.

González-Vallinas, M., González-Castejón, M., Rodríguez-Casado, A., Ramírez de Molina, A. (2013). Dietary phytochemicals in cancer prevention and therapy: a complementary approach with promising perspectives. *Nutrition Reviews, 71*, 585-599.

Kang, K.A., Piao, M.J., Ryu, Y.S., Hyun, Y.J., Park, J.E., Shilnikova, K., Zhen, A.X., Kang, H.K., Koh, Y.S., Jeong, Y.J. (2017). Luteolin induces apoptotic cell death via antioxidant activity in human colon cancer cells. *International Journal of Oncology, 51,*1169-1178.

Kee, J.Y., Han, Y.H., Kim, D.S., Mun, J.G., Park, J., Jeong, M.Y., Um, J.Y., Hong, S.H. (2016). Inhibitory effect of quercetin on colorectal lung metastasis through inducing apoptosis, and suppression of metastatic ability. *Phytomedicine, 23,* 1680-1690.

Khan, I., Paul, S., Jakhar, R., Bhardwaj, M., Han, J., Kang, S.C. (2016). Novel quercetin derivative TEF induces ER stress and mitochondria-mediated apoptosis in human colon cancer HCT-116 cells. *Biomedicine & Pharmacotherapy, 84,* 789-799.

Kim, M.E., Ha, T.K., Yoon, J.H., Lee, J.S. (2014). Myricetin induces cell death of human colon cancer cells via BAX/BCL2-dependent pathway. *Anticancer Research, 34,* 701-706.

Kishore, R.K., Halim, A.S., Syazana, M.S.N., Sirajudeen, K.N.S. (2011). Tualang honey has higher phenolic content and greater radical scavenging activity compared with other honey sources. *Nutrition Research, 31,* 322-325.

Lee, K.W., Bode, A.M., Dong, Z. (2011). Molecular targets of phytochemicals for cancer prevention. *Nature Reviews Cancer, 11*, 211-218.

Nishida, C., Uauy, R., Kumanyika, S., & Shetty, P. (2004). The joint WHO/FAO expert consultation on diet, nutrition and the prevention of chronic diseases: process, product and policy implications. *Public health nutrition*, 7, 245-250.

Nicholson, D. W., Ali, A., Thornberry, N. A., Vaillancourt, J. P., Ding, C. K., Gallant, M., ... & Munday, N. A. (1995). Identification and inhibition of the ICE/CED-3 protease necessary for mammalian apoptosis. *Nature*, 376, 37.

Núñez-Sánchez, M.A., González-Sarrías, A., Romo-Vaquero, M., García-Villalba, R., Selma, M.V., Tomás-Barberán, F.A., García-Conesa, M.T., Espín, J.C. (2015). Dietary phenolics against colorectal cancer—From promising preclinical results to poor translation into clinical trials: Pitfalls and future needs. *Molecular Nutrition & Food Research, 59,* 1274-1291.

Pandey, K.B., Rizvi, S.I. (2009). Plant polyphenols as dietary antioxidants in human health and disease. *Oxidative Medicine and Cellular Longevity*, *2*, 270-278.

Petretto, G.L., Cossu, M., Alamanni, M.C. (2015). Phenolic content, antioxidant and physico-chemical properties of Sardinian monofloral honeys. *International Journal of Food Science & Technology, 50*, 482-491.

Phang C.W., Karsani S.A., Sethi G., Malek. (2016). Flavokawain C inhibits cell cycle and promotes apoptosis, associated with endoplasmic reticulum stress and regulation of MAPKs and Akt signaling pathways in HCT 116 human colon carcinoma cells. *PLoS One, 11,* e0148775.

Pino, M.S., Chung D.C. (2010). The chromosomal instability pathway in colon cancer. *Gastroenterology*, *138,* 2059-2072.

Reddy, B.S. (2018). Diet and colon cancer: evidence from human and animal model studies. Diet, Nutrition and Cancer: A Critical Evaluation, pp. 47-65. Boca Raton, FL: CRC Press, 1986, Place Published, 2018.

Rosa, A., Tuberoso, C.I.G., Atzeri, A., Melis, M.P., Bifulco E., Dessì, M.A. (2011). Antioxidant profile of strawberry tree honey and its marker homogentisic acid in several models of oxidative stress. *Food Chemistry, 129,* 1045-1053.

Sano, R., Reed, J.C. (2013). ER stress-induced cell death mechanisms. *Biochimica et Biophysica Acta, 1833,* 3460-3470.

Scanu, R., Spano, N., Panzanelli, A., Pilo, M.I., Piu, P.C., Sanna, G., Tapparo, A. (2005). Direct chromatographic methods for the rapid determination of homogentisic acid in strawberry tree (Arbutus unedo L.) honey. *Journal of Chromatography A, 1090,* 76-80.

Siegel, R.L., Miller, K.D., Fedewa, S.A., Ahnen, D.J., Meester, R.G.S., Barzi, A., Jemal, A. (2017). Colorectal cancer statistics. *CA Cancer Journal for Clinicians, 67,* 177-193.

Sun, C., Tan, H., Zhang, Y., Zhang, H. (2016). Phenolics and abscisic acid identified in acacia honey comparing different SPE cartridges coupled with HPLC-PDA. *Journal of Food Composition and Analysis, 53,* 91-101.

Tang, H., Yao, X., Yao, C., Zhao, X., Zuo, H., Li, Z. (2017). Anti-colon cancer effect of caffeic acid p-nitro-phenethyl ester in vitro and in vivo and detection of its metabolites, *Scientific Reports, 7,* 7599.

Tuberoso, C.I.G., Boban, M., Bifulco, E., Budimir, D., Pirisi, F.M. (2013). Antioxidant capacity and vasodilatory properties of Mediterranean food: the case of Cannonau wine, myrtle berries liqueur and strawberry-tree honey. *Food Chemistry, 140,* 686-691.

Vermeulen K., Van Bockstaele D.R., Berneman Z.N. (2003). The cell cycle: a review of regulation, deregulation and therapeutic targets in cancer. *Cell Proliferation, 36,* 131-149.

Wang, J., Fang, X., Ge, L., Cao, F., Zhao, L., Wang, Z., Xiao W. (2018). Antitumor, antioxidant and anti-inflammatory activities of kaempferol and its corresponding glycosides and the enzymatic preparation of kaempferol. *PLoS One, 13,* e0197563.

Wang, W., Heideman, L., Chung, C.S., Pelling, J.C., Koehler, K.J., Birt, D.F. (2000). Cell-cycle arrest at G2/M and growth inhibition by apigenin in human colon carcinoma cell lines. *Molecular Carcinogenesis, 28,* 102-110.

Wen, C.T.P., Hussein, S.Z., Abdullah, S., Karim, N.A., Makpol, S., Yusof, Y.A.M. (2012). Gelam and nenas honeys inhibit proliferation of HT29 colon cancer cells by inducing DNA damage and apoptosis while suppressing inflammation. *Asian Pacific Journal of Cancer Prevention, 13,* 1605-1610.

Wu, J., Omene, C., Karkoszka, J., Bosland, M., Eckard, J., Klein, C.B., Frenkel, K. (2011). Caffeic acid phenethyl ester (CAPE), derived from a honeybee product propolis, exhibits a diversity of anti-tumor effects in pre-clinical models of human breast cancer. *Cancer Letters, 308,* 43-53.

Wu, W., Guo, F., Ye, J., Li, Y., Shi, D., Fang, D., Guo, J., Li, L. (2016). Pre-and post-diagnosis physical activity is associated with survival benefits of colorectal cancer patients: a systematic review and meta-analysis. *Oncotarget, 7,* 52095.

Zhang, W., Liu, H.T. (2002). MAPK signal pathways in the regulation of cell proliferation in mammalian cells. *Cell Research, 12,* 9-18.

Figure Legends

Figure 1. DAD-chromatogram in full-scan mode (range between 200 and 600 nm) for the determination of (A) phenolic compounds in STH; (B) Flavonols; (C) Phenolic acids. Peak identification: Flavonols: (1) Rutin; (2) Myricetin; (3) Fisetin; (4) Quercetin; (5) Luteolin; (6) Apigenin; (7) Kaempferol; (8) Isorhammetin; Phenolic acids: (9) Gallic acid; (10) Protocatechuic acid; (11) 4-Hydroxybenzoic acid; (12) Vanillic acid; (13) Caffeic acid; (14) Syringic acid; (15) p-coumaric acid; (16) trans-ferulic acid; (17) Ellagic acid; (18) trans-cinnamic acid.

Figure 2. Effect of STH in HCT-116, LoVo and non-cancer cells proliferation. (A) HCT-116, (B) LoVo and (C) non-cancer cells were pre-treated with different concentrations of STH for 24, 48 and 72 h, and the cell viability was assayed by MTT assay. Results were expressed as percentage (%) of viable cells compared to untreated cells and showed mean ± standard deviation (SD). n=3.

Figure 3. Effect of STH in HCT-116, LoVo and non-cancer cells colony formation. The cells were seeded at low density in McCoy's 5A, F-12 K and DMEM media supplements with or without different concentrations of STH for 12 days. The results were expressed as a % of the colonies that corresponds to untreated cells. The colonies were fixed with 70% ethanol and stained with methyleneblue for the analysis of colony formation. Quantitative image analysis of colonies in cultured (A) HCT-116, (B) LoVo and (C) non-cancer cells. Results expressed as the mean ± SD (n = 3). $*p< 0.05$; $**p< 0.01$ vs. control group. $^{\#}p< 0.05$; $^{\#\#}p< 0.01$ vs. treatment group.

Figure 4. Cell cycle analysis after the treatment of STH in HCT-116 and LoVo cells. Images represent an example of the response of (A) HCT-116 and (B) LoVo cells with or without different concentrations of STH for 48 h. Percentages in each cell cycle phase (G1, S and G2/M) are presented in the bar diagram. Results expressed as the mean ± SD (n = 3). *p< 0.05; **p< 0.01 vs. control group. #p< 0.05; ##p< 0.01 vs. treatment group.

Figure 5. Effect of STH on cell cycle regulatory mRNA levels in HCT-116 and LoVo cells. (A) HCT-116 and (B) LoVo cells were pre-treated with or without different concentrations of STH for 48 h. Cyclin D1, cyclin E, CDK2, CDK4, p21Cip, p27Kip and p-Rb mRNA levels were analyzed by RT-PCR and the data were normalized by GADPH mRNA levels. Results are expressed as median, first quartiles, third quartiles, minimum and maximum values and expressed as the mean ± SD (n = 3). *p< 0.05; **p< 0.01 vs. control group. #p< 0.05; ##p< 0.01 vs. treatment group.

Figure 6. Effect of STH on apoptosis induction in HCT-116 and LoVo cells. (A) HCT-116, (B) LoVo and (C) non-cancer cells were pre-treated with or without different concentrations of STH for 48 h. Tali™ Image-based Cytometer were used for calculating the number of viable, death and apoptotic cells after Annexin V Alexa Fluor® 488 and PI staining. Fluorescence image shows the effect of STH with or without treatment: blue color represents live cells, green color represents apoptotic cells and red and yellow colors represent dead cells. Results are expressed as the mean ± SD (n = 3). *p< 0.05; **p< 0.01 vs. control group. $^{\#}p$< 0.05; $^{\#\#}p$< 0.01 vs. treatment group. *Scale bar* 50 μm.

Figure 7. Effect of STH on intrinsic and extrinsic apoptotic related signaling mRNA levels in HCT-116 and LoVo cells. (A) HCT-116 and (B) LoVo cells were pre-treated with or without different concentrations of STH for 48 h. p53, Bax/Bcl2, Cyto C, Fas L, caspase-3, -8, -9 and c-PARP mRNA levels were analyzed by RT-PCR and the data were normalized by GADPH mRNA levels. Results are expressed as median, first quartiles, third quartiles, minimum and maximum values and expressed as the mean ± SD (n = 3). *p< 0.05; **p< 0.01 vs. control group. $^{\#}p$< 0.05; $^{\#\#}p$< 0.01 vs. treatment group.

Figure 8. Effect of STH on apoptotic and ER stress proteins in HCT-116 and LoVo cells. Cells were pre-treated with or without different concentrations of STH for 48 h. The apoptotic proteins p53, caspase-3 and c-PARP expression was determined by immunoblotting in (A) HCT-116 and (B) LoVo cells (normalized to GADPH loading control). Similarly, the ER stress protein ATF-6 and XBP1 expression were determined by immunoblotting in (C) HCT-116 and (D) LoVo cells (normalized to GADPH loading control). Results are expressed as median, first quartiles, third quartiles, minimum and maximum values and expressed as the mean ± SD (n = 3). *p< 0.05; **p< 0.01 vs. control group. $^{\#}p$< 0.05; $^{\#\#}p$< 0.01 vs. treatment group.

Figure 9. Effect of STH on EGFR and MAPK signaling in HCT-116 and LoVo cells. Cells were pre-treated with or without different concentrations of STH for 48 h. The marker of EGFR signaling (EGFR, HER2, p-Akt and p-mTOR) in (A) HCT-116 and LoVo (B) cells, and the marker of MAPK signaling (p-p38MAPK and p-ERK1/2) in (C) HCT-116 and LoVo (D) cells expression were determined by immunoblotting in HCT-116 and LoVo cells (normalized to GADPH loading control). Results are expressed as median, first quartiles, third quartiles, minimum and maximum

values and expressed as the mean ± SD (n = 3). *p< 0.05; **p< 0.01 vs. control group. $^{\#}p$< 0.05; $^{\#\#}p$< 0.01 vs. treatment group.

Table Captions.

Table 1. The sequences of real-time PCR oligonucleotide primers.

Table 2. CAS number, retention time (RT, min), maximum absorption wavelengths (λ, nm) and concentration (mg/100 g of honey) for the considered phenolic compounds determined in Strawberry Tree Honey (STH).

Table 3. Total antioxidant capacity of Strawberry tree honey.

Figure 1

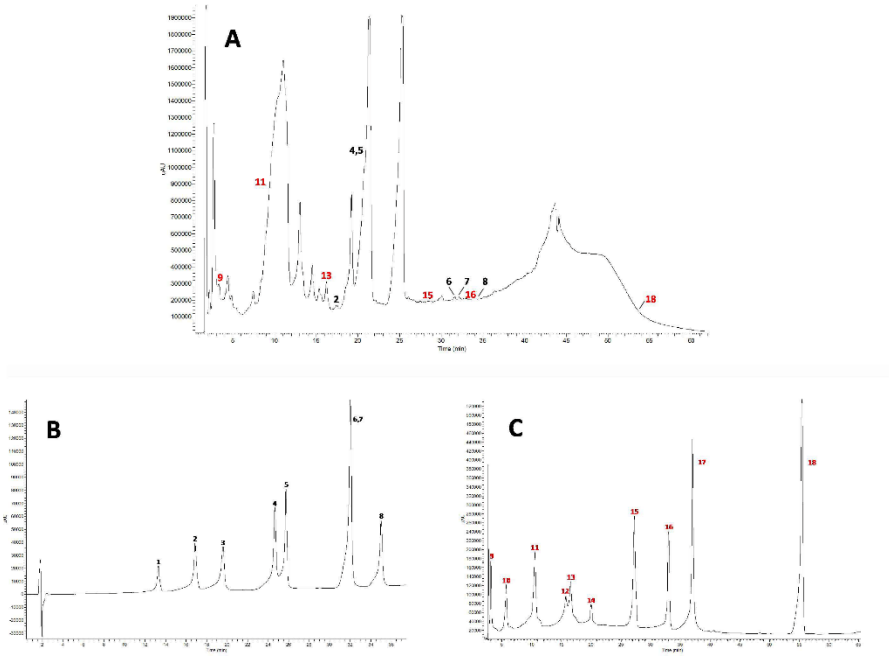

Figure 2

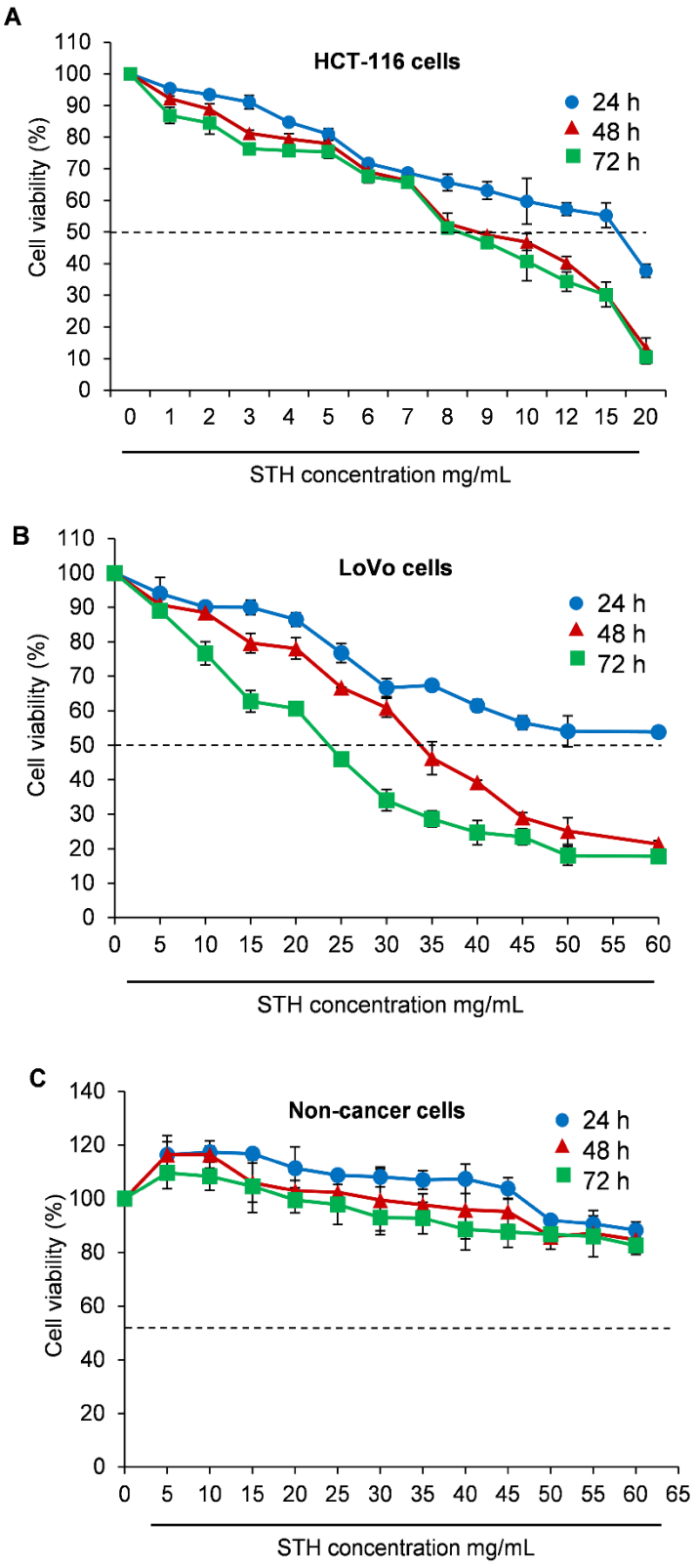
A
HCT-116 cells
24 h
48 h
72 h
Cell viability (%)
STH concentration mg/mL
B
LoVo cells
24 h
48 h
72 h
Cell viability (%)
STH concentration mg/mL
C
Non-cancer cells
24 h
48 h
72 h
Cell viability (%)
STH concentration mg/mL

Figure 3

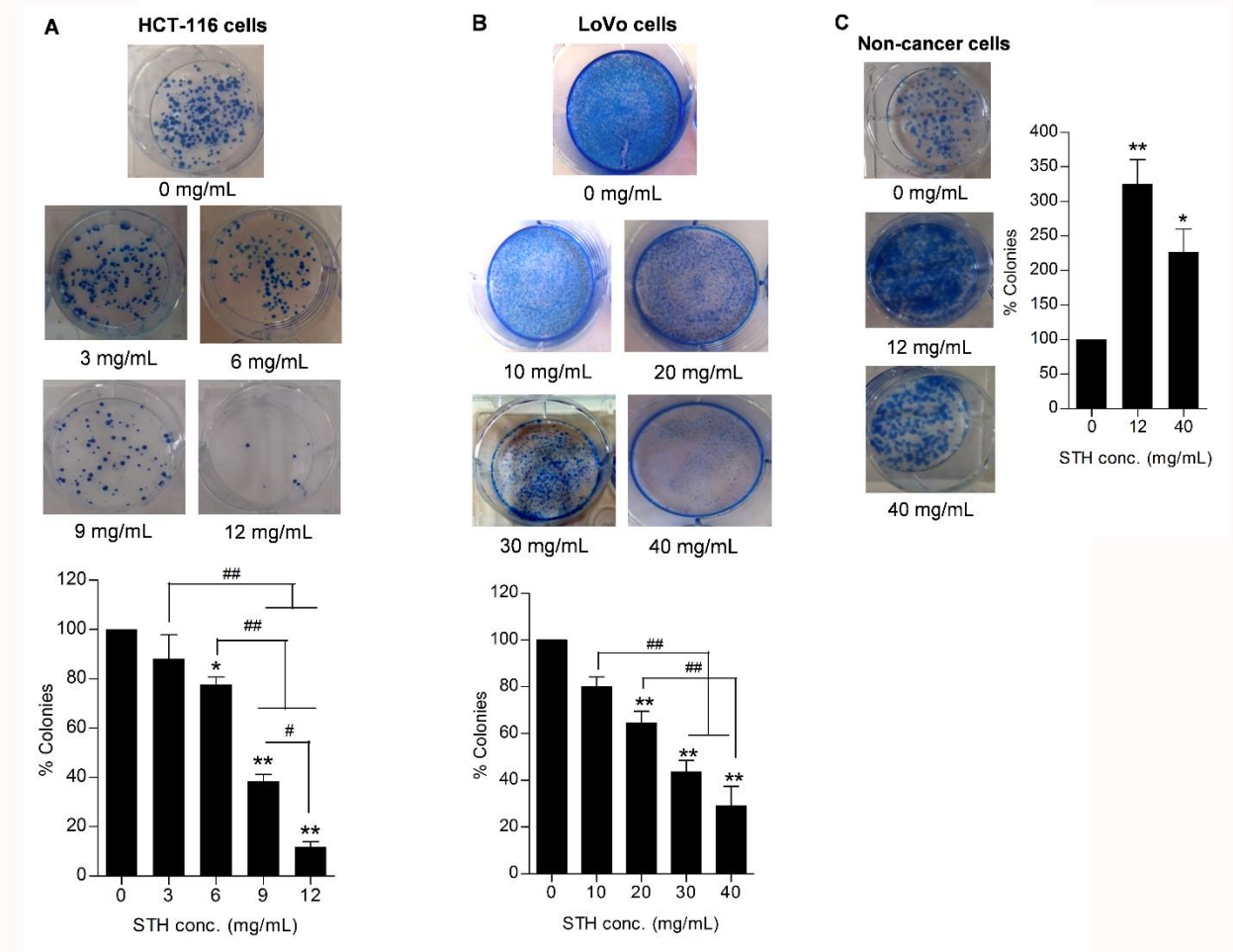
A
HCT-116 cells
0 mg/mL
3 mg/mL
6 mg/mL
9 mg/mL
12 mg/mL
% Colonies
STH conc. (mg/mL)
B
LoVo cells
0 mg/mL
10 mg/mL
20 mg/mL
30 mg/mL
40 mg/mL
% Colonies
STH conc. (mg/mL)
C
Non-cancer cells
0 mg/mL
12 mg/mL
40 mg/mL
% Colonies
STH conc. (mg/mL)

Figure 4

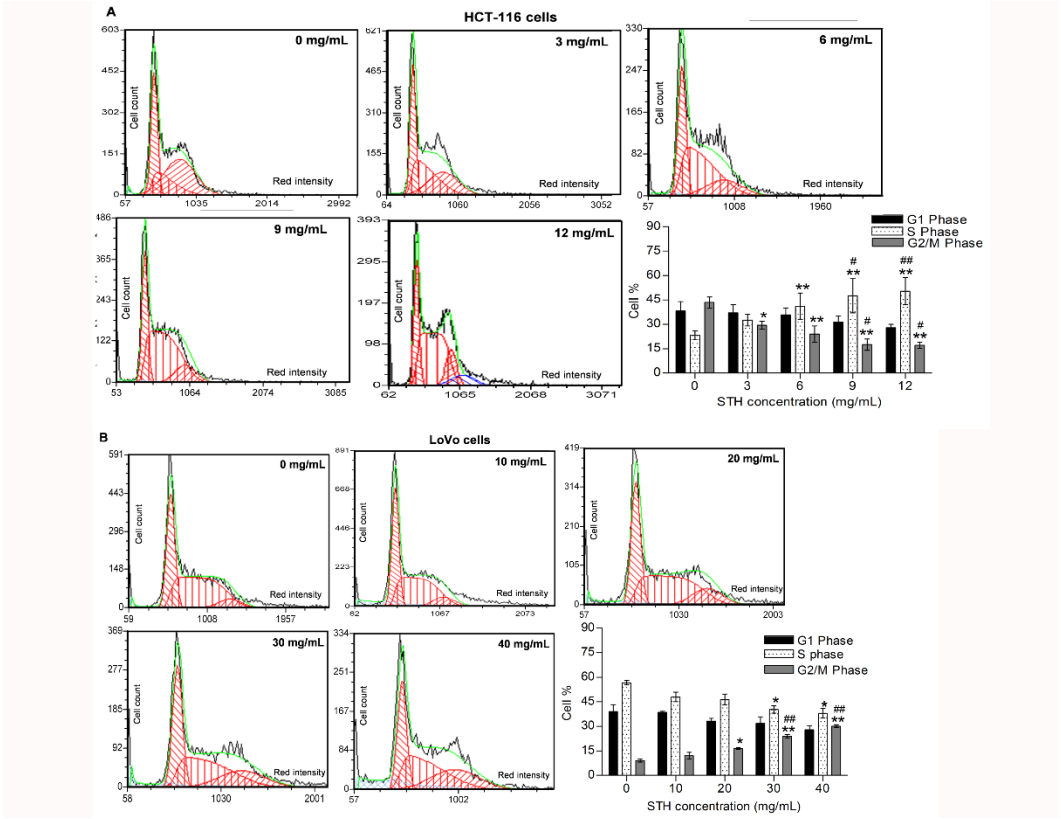
A
HCT-116 cells
0 mg/mL
3 mg/mL
6 mg/mL
9 mg/mL
12 mg/mL
Cell count
Red intensity
G1 Phase
S Phase
G2/M Phase
Cell %
STH concentration (mg/mL)
B
LoVo cells
0 mg/mL
10 mg/mL
20 mg/mL
30 mg/mL
40 mg/mL
G1 Phase
S phase
G2/M Phase
Cell %
STH concentration (mg/mL)

Figure 5

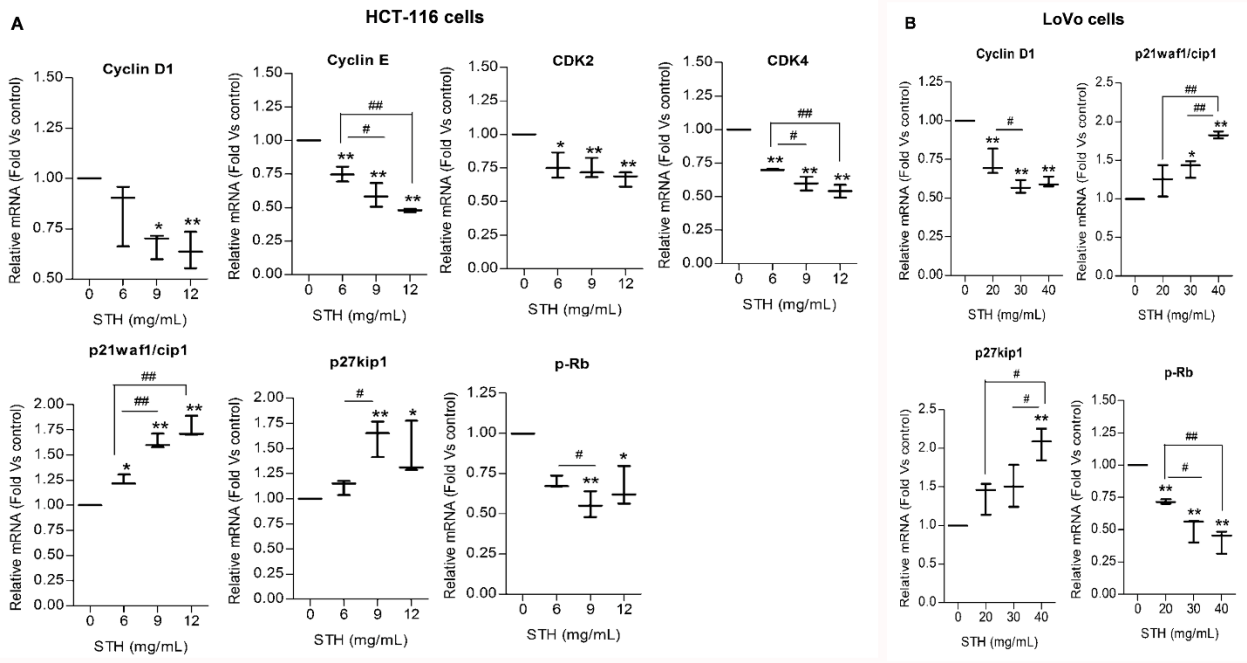
A
HCT-116 cells
Cyclin D1
Cyclin E
CDK2
CDK4
p21waf1/cip1
p27kip1
p-Rb
Relative mRNA (Fold Vs control)
STH (mg/mL)
B
LoVo cells
Cyclin D1
p21waf1/cip1
p27kip1
p-Rb
Relative mRNA (Fold Vs control)
STH (mg/mL)

Figure 6

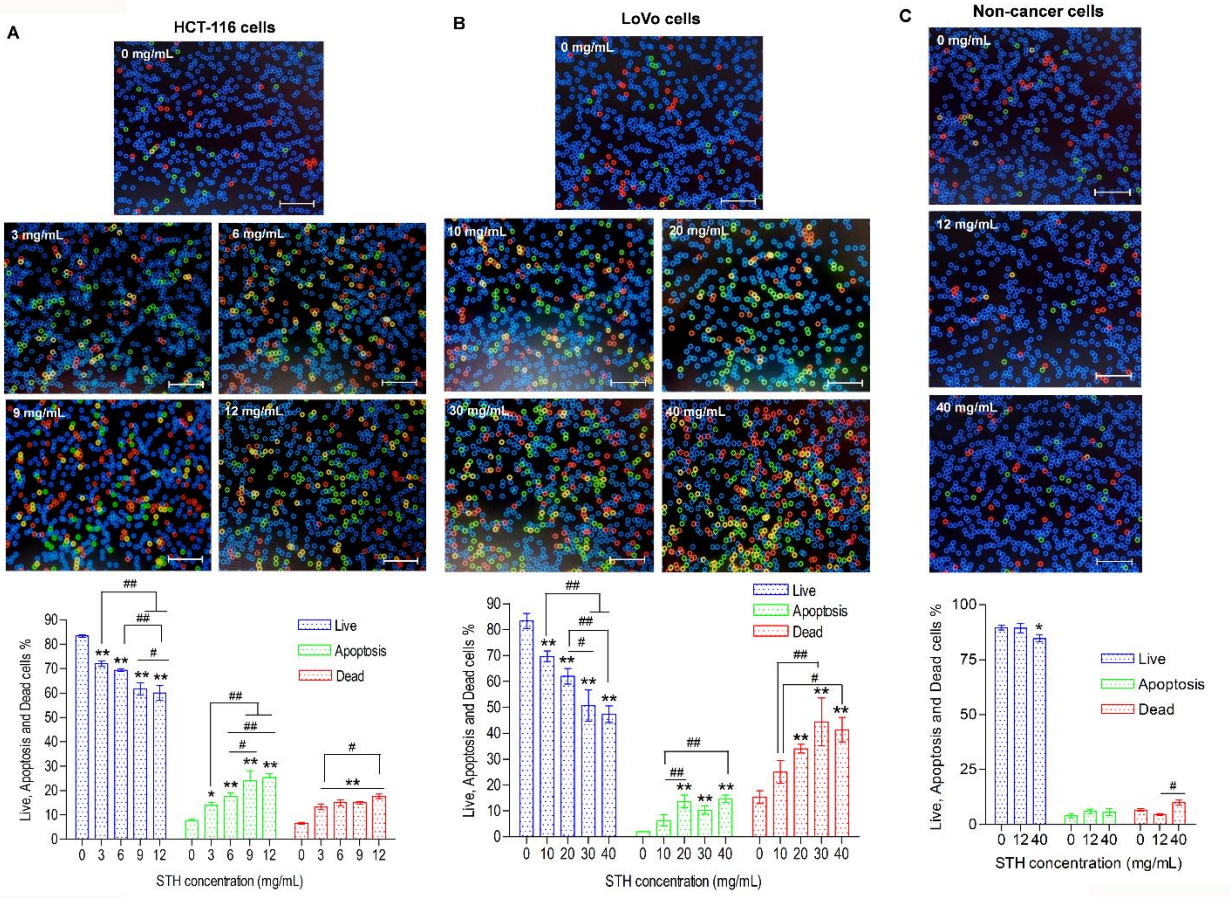
A
HCT-116 cells
0 mg/mL
3 mg/mL
6 mg/mL
9 mg/mL
12 mg/mL
B
LoVo cells
0 mg/mL
10 mg/mL
20 mg/mL
30 mg/mL
40 mg/mL
C
Non-cancer cells
0 mg/mL
12 mg/mL
40 mg/mL
Live
Apoptosis
Dead
Live, Apoptosis and Dead cells %
STH concentration (mg/mL)

Figure 7

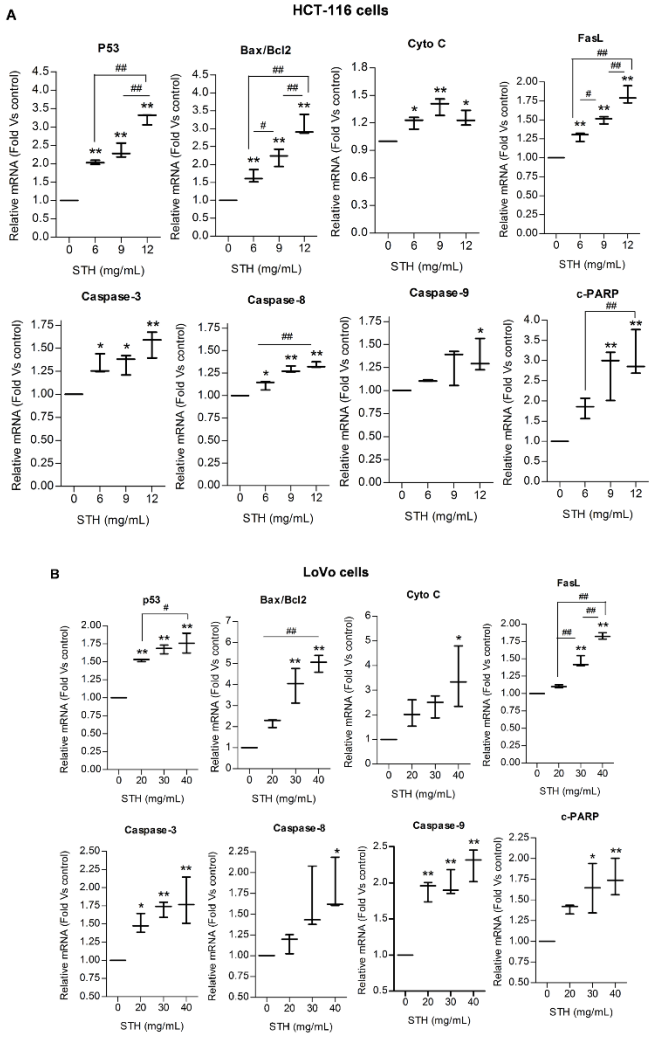
A
HCT-116 cells
P53
Bax/Bcl2
Cyto C
FasL
Caspase-3
Caspase-8
Caspase-9
c-PARP
Relative mRNA (Fold Vs control)
STH (mg/mL)
B
LoVo cells
p53
Bax/Bcl2
Cyto C
FasL
Caspase-3
Caspase-8
Caspase-9
c-PARP
Relative mRNA (Fold Vs control)
STH (mg/mL)

Figure 8

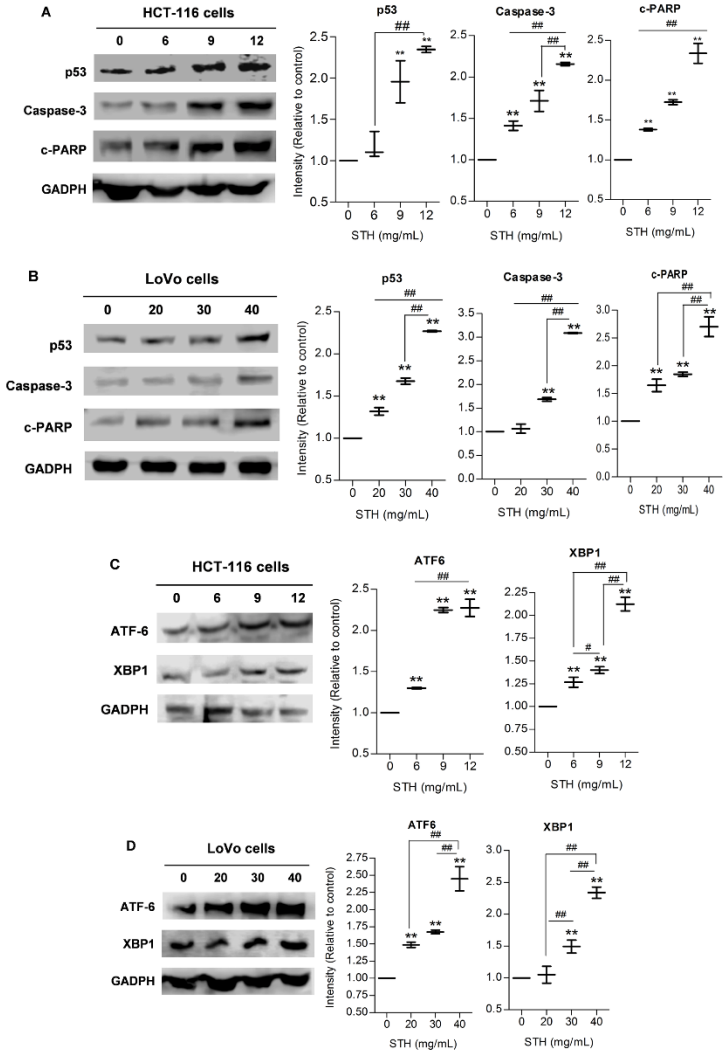
A
HCT-116 cells
0 6 9 12
p53
Caspase-3
c-PARP
GADPH
p53
Caspase-3
c-PARP
Intensity (Relative to control)
STH (mg/mL)
B
LoVo cells
0 20 30 40
p53
Caspase-3
c-PARP
GADPH
C
HCT-116 cells
ATF-6
XBP1
GADPH
ATF6
XBP1
D
LoVo cells

Figure 9

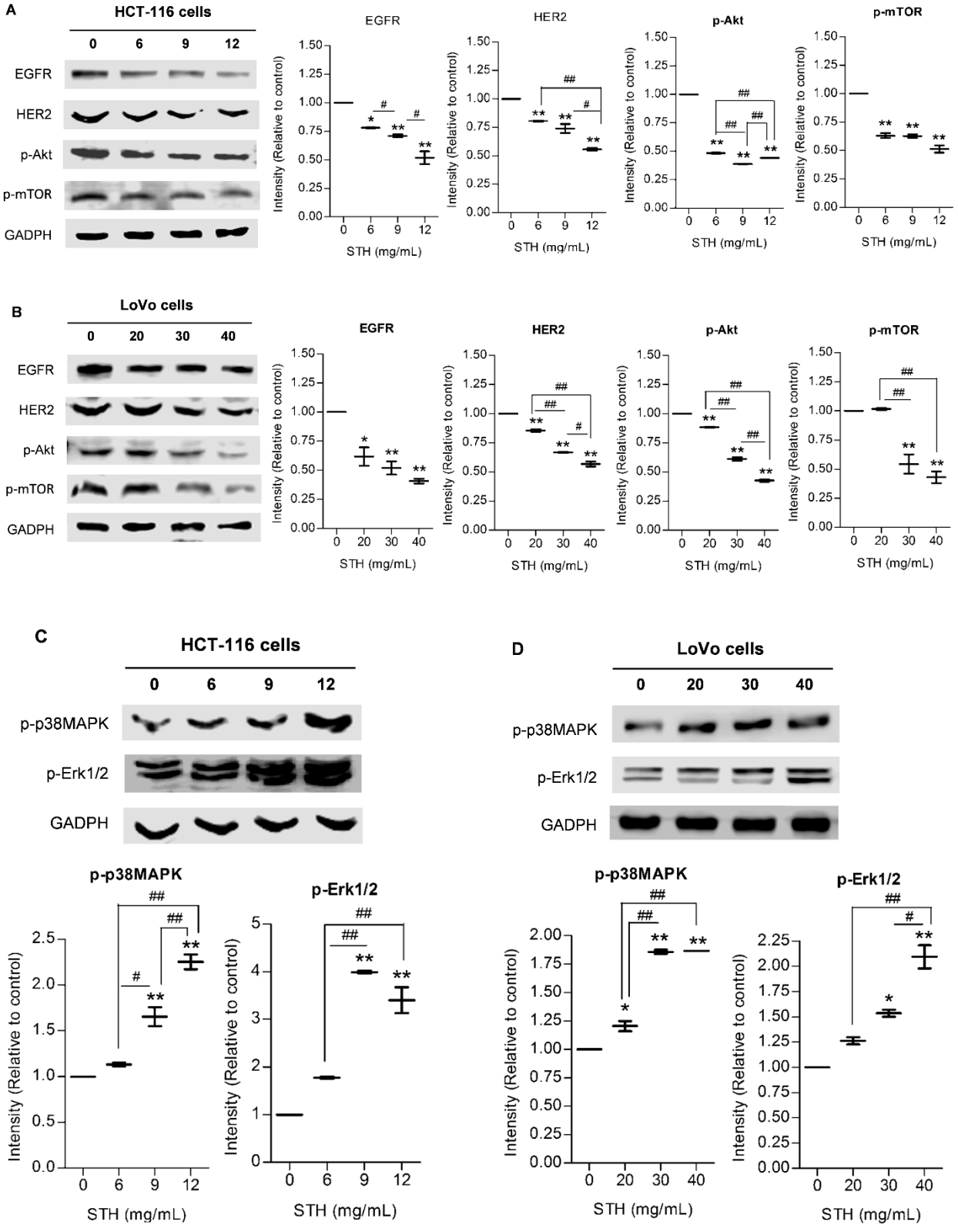
A
HCT-116 cells
0 6 9 12
EGFR
HER2
p-Akt
p-mTOR
GADPH
EGFR
HER2
p-Akt
p-mTOR
Intensity (Relative to control)
STH (mg/mL)
B
LoVo cells
0 20 30 40
EGFR
HER2
p-Akt
p-mTOR
GADPH
C
HCT-116 cells
0 6 9 12
p-p38MAPK
p-Erk1/2
GADPH
p-p38MAPK
p-Erk1/2
D
LoVo cells
0 20 30 40
p-p38MAPK
p-Erk1/2
GADPH
p-p38MAPK
p-Erk1/2

Table 1. The sequences of real-time PCR oligonucleotide primers.

Gene	Direction	Sequence (5′-3′)
p53	Forward	AGACCTATGGAAACTGTGAGTGGA
	Reverse	GAAGCCTAAGGGTGAAGAGGA
Caspase-3	Forward	CTGGACTGTGGCATTGAGACA
	Reverse	CGGCCTCCACTGGTATTTTATG
c-PARP	Forward	GGGAGGAGATGGAATGTCAG
	Reverse	CTGCTGGGTCCAAAAGAGAC
Bcl-2	Forward	CCTGTGGATGACTGAGTACC
	Reverse	GAGACAGCCAGGAGAAATCA
Bax	Forward	GTTTCATCCAGGATCGAGCAG
	Reverse	CATCTTCTTCCAGATGGTGA
Cyt C	Forward	TTTGGATCCAATGGGTGATGTTGAG
	Reverse	CCATCCCTACGCATCCTTTAC
Fas L	Forward	GGATTGGGCCTGGGGATGTTTCA
	Reverse	TTGTGGCTCAGGGGCAGGTTGTTG
Caspase-8	Forward	AGAGTCTGTGCCCAAATCAAC
	Reverse	GCTGCTTCTCTCTTTGCTGAA
Caspase-9	Forward	TGTCCTACTCTACTTTCCCAGTTTT
	Reverse	GAGACAGCCAGGAGAAATCA
Cyclin D1	Forward	GAACAAACAGATCATCCGCAA
	Reverse	TGCTCCTGGCAGGCACGGA
Cyclin E	Forward	GAGCCAGCCTTGGGACAATAA
	Reverse	GCACGTTGAGTTTGGGTAAACC
CDK2	Forward	TTTGCTGAGTGGTGACTCGCCG
	Reverse	CCGGCCCACTTGGGGAAAC
CDK4	Forward	CTTCCCGTCAGCACAGTTC
	Reverse	GGTCAGCATTTCCAGTAGC
p21waf1/cip1	Forward	GCGATGGAACTTCGACTTTGT
	Reverse	GGGCTTCCTCTTGGAGAAGAT
p27kip1	Forward	ATGTCAAACGTGCGAGTGTC
	Reverse	TCTCTGCAGTGCTTCTCCA
p-Rb	Forward	ATCCGAGGCAACTACAGCCTA
	Reverse	CCTTTCCAACCGTGGGAATAAT
GADPH	Forward	GACCCCTTCATTGACCTCAACTACATG
	Reverse	GTGCACCACCCTGTTGCTGTAGCC

Table 2. CAS number, retention time (RT, min), maximum absorption wavelengths (λ, nm) and concentration (mg/100 g of honey) for the considered phenolic compounds determined in Strawberry Tree Honey (STH).

Phenolic compounds	CAS number	RT (min)	λ (nm)	Concentration (mg/100g of honey)
Flavonols				
Rutin	153-18-4	13.34	352	nd
Myricetin	529-44-2	17.07	368	0.61±0.04
Fisetin	528-48-3	19.73	361	nd
Quercetin	117-39-5	24.65	371	0.90±0.02
Luteolin	491-70-3	25.69	347	0.79±0.10
Apigenin	520-36-5	31.91	337	0.19±0.06
Kaempferol	520-18-3	31.93	365	1.90±0.05
Isorhammetin	480-19-3	34.83	370	0.23±0.07
Total flavonols content				*4.62*
Phenolic acids				
Gallic acid	149-91-7	3.11	270	3.92±0.16
Protocatechuic acid	99-50-3	5.65	259	nd
4-Hydroxybenzoic acid	99-96-7	10.52	254	1.29±0.02
Vanillic acid	121-34-6	15.65	260	nd
Caffeic acid	331-39-5	16.54	322	1.22±0.06
Syringic acid	530-57-4	19.87	274	nd
p-coumaric acid	501-98-4	27.46	308	0.10±0.03
trans-ferulic acid	537-98-4	33.19	322	0.53±0.00
Ellagic acid	476-66-4	38.08	251	nd
trans-cinnamic acid	140-10-3	55.88	273	0.14±0.01
Total phenolic acid content				*7.20*

nd: not detected. Data are means (n=3).

Table 3. Total antioxidant capacity of Strawberry tree honey.

Parameter	**Quantification**
TEAC Values (µmol TE/100 g)	392.13±0.45
FRAP Values (µmol TE/100 g)	539.01±0.27
DPPH Values (µmol TE/100 g)	200.83±0.68

Graphical abstract